





## Article

# Techno-Economic Assessment of Producer Gas from Heavy Oil and Biomass Co-Gasification Aiming Electricity Generation in Rankine Cycle

York Castillo Santiago <sup>1,\*</sup>, Nelson Calderon Henao <sup>2</sup>, Osvaldo José Venturini <sup>2</sup>, Leandro A. Sphaier <sup>1</sup>, Stefany Vera Duarte <sup>3</sup>, Túlio Tito Godinho de Rezende <sup>2</sup> and Guillermo Valencia Ochoa <sup>3</sup>

<sup>1</sup> Laboratory of Thermal Sciences (LATERMO), Department of Mechanical Engineering (TEM/PGMEC), Fluminense Federal University (UFF), Rua Passo da Pátria 156, Niterói 24210-240, Brazil

<sup>2</sup> Excellence Group in Thermal Power and Distributed Generation (NEST), Federal University of Itajubá (UNIFEI), Av. BPS 1303, Itajubá 37500-903, Brazil

<sup>3</sup> Efficient Energy Management Group (KAI), Department of Mechanical Engineering, Universidad del Atlántico, Carrera 30 # 8–49, Puerto Colombia 081001, Colombia

\* Correspondence: yorkcastillo@id.uff.br

**Abstract:** Heavy oil and biomass co-gasification has been analyzed through a model developed in Aspen Plus™ v 11.0 software. The model was used to assess main gasification parameters, such as cold gas efficiency, yield, low heating value (LHV), and producer gas composition, using air and oxygen as gasification agents. Subsequently, producer gas energy use in the Rankine cycle was performed using a model developed in GateCycle™ v11.1.2.4.850 software. Likewise, the economic indicators of the integrated Rankine cycle-gasification system were calculated. The economic evaluation was developed through Monte Carlo simulation using Crystalball™. The results showed a LHV producer gas decreasing trend as the equivalence ratio (ER) increased, oscillating between 6.37 and 3.63 MJ/Nm<sup>3</sup> for ER values greater than 0.30 in the air co-gasification case, while the scenario that used oxygen presented better LHV results, ranging from 9.40 to 11.79 MJ/Nm<sup>3</sup>. For air co-gasification, the Rankine cycle efficiency range was between 13.0% and 9.5%, while for oxygen co-gasification, values between 14.0% and 13.2% were obtained. Regarding the economic assessment, the two scenarios evaluated (with a reliability of 95%) have a probability higher than 92.1% of economic losses due mainly to the lower electrical power and the local electricity rate.

**Keywords:** heavy oil; biomass; gasification; economic assessment; Rankine cycle; electricity generation



**Citation:** Castillo Santiago, Y.; Henao, N.C.; Venturini, O.J.; Sphaier, L.A.; Duarte, S.V.; de Rezende, T.T.G.; Ochoa, G.V. Techno-Economic Assessment of Producer Gas from Heavy Oil and Biomass Co-Gasification Aiming Electricity Generation in Rankine Cycle. *Processes* **2022**, *10*, 2358. <https://doi.org/10.3390/pr10112358>

Academic Editor: Paola Ammendola

Received: 15 October 2022

Accepted: 7 November 2022

Published: 11 November 2022

**Publisher's Note:** MDPI stays neutral with regard to jurisdictional claims in published maps and institutional affiliations.



**Copyright:** © 2022 by the authors. Licensee MDPI, Basel, Switzerland. This article is an open access article distributed under the terms and conditions of the Creative Commons Attribution (CC BY) license (<https://creativecommons.org/licenses/by/4.0/>).

## 1. Introduction

According to the Organization of Petroleum Exporting Countries, oil demand will increase by 16.4 MB/day between 2015 and 2040, corresponding to 99.2 MB/day in 2021 and 109.4 MB/day in 2040 [1]. Light crude oil reserves have been consumed excessively over the past decades. Therefore, unconventional resources, such as heavy oil, have been considered fuel alternatives [2]. Heavy oil is a dense, viscous, and asphaltic oil that contains asphaltenes and has an American Petroleum Institute (API) density ranging between 10° and 20° API [3]. Heavy crude oil is a complicated mixture of different hydrocarbons divided into four major components: saturates, aromatic, resin, and asphaltene (SARA) [4]. Recently, in situ upgrading methods have been developed for oil product use, such as solvent-based and in situ thermochemical conversion (pyrolysis and gasification), among others. These methods aim to process heavy crude oil using three mechanisms: increasing short-chain hydrocarbons, reducing asphaltene, and removing heteroatoms [5].

Biomass for energy use is generated from different sources, such as wood, agricultural, food, and petroleum refinery residues, which could be converted into bioproducts through thermochemical conversion processes, viz. pyrolysis, carbonization, gasification, among

others [6]. Some petroleum refineries in Brazil occupy large areas with extensive vegetation (trees and lawns) due to the oil production process (refining, transportation, processing, and distribution) and oily residue generation [7,8]. Thus, pruning trees and lawns is a daily activity in the refineries, producing biomass that requires proper disposal, and one of the possibilities is its energy use. According to González-Arias et al. [9], biomasses pruning shows potential for energy recovery, but those are usually scattered in fields or eliminated by burning. Pyrolysis is the thermal degradation of carbonaceous materials in the absence of oxygen, converting biomass to bio-oil, char, and non-condensable gases [10]. After hydrotreatment and upgrading, the bio-oil obtained from by-products pyrolysis (such as biomass and heavy oil) will have properties comparable to those produced at the same refinery [11,12].

On the other hand, gasification is the thermal decomposition process of a carbon-rich raw material under an oxidizing atmosphere that aims to produce fuel gases with energy potential from removing volatiles from the fuel's carbon matrix. The gasification process requires a gasification agent, which allows the molecular structure of the raw material to be rearranged [13]. For this purpose, steam, oxygen, air, carbon dioxide, hydrogen, or a mixture are usually used. The gasification agent reacts with char and heavier hydrocarbons during the process, transforming them into low molecular weight gases, such as CO and H<sub>2</sub> [14]. Subsequently, producer gas is generated and, after being conditioned, can be used directly as fuel in prime movers, such as internal combustion engines, gas microturbines, or Rankine cycles [15].

Ghassemi et al. [16] studied the gasification of extra-heavy oil using a model based on the Gibbs free energy minimization approach. The authors observed that an increase in equivalence ratio (ER) from 0.2 to 0.8 leads to a considerable decrease in the higher heating value (HHV) of producer gas (from 15.2 to 4.7 MJ/Nm<sup>3</sup>) and in the cold efficiency (80% to 47%), while the char conversion efficiency increases from 43% to 92%. Yang et al. [17] modeled the heavy oil gasification process in Aspen Plus<sup>TM</sup> software, considering mixtures of air and steam as gasification agents. The results showed that temperature plays an essential role in the process, where gasification temperature of 800 °C produced the highest H<sub>2</sub> yield (58 g H<sub>2</sub>/kg-fuel). They also found that using a steam/oil ratio of 0.7 could cause a significant increase in H<sub>2</sub> yield.

Bader et al. [18] numerically evaluated the gasification of heavy oil using O<sub>2</sub> and steam mixtures as a gasification agent. The authors developed a computational fluid dynamics model that comprises the implementation of heterogeneous char reactions in ANSYS Fluent<sup>TM</sup> v17.2 software, obtaining a producer gas at a temperature of 1599 K and with 50.55% CO, 42.71% H<sub>2</sub>, 3.55% CO<sub>2</sub>, and 0.54% CH<sub>4</sub>; demonstrating that the impact of the producer gas composition on oil conversion is smaller when the humidity decreases. Banisaeed and Rezaee-Manesh [19] developed a kinetic model of heavy oil gasification to investigate the influence of oxygen as a gasification agent and pressure on producer gas composition and yield. The results indicated that an increase of 0.4 to 1.0 in the oxygen ratio leads to increases in the HHV value and in the cold efficiency of the gasification process, which increase from 8.0 to 10.0 MJ/Nm<sup>3</sup> and from 35% to 70%, respectively. On the other hand, the authors observed that increases in the gasification pressure from 10 to 40 atm did not influence the HHV and yield of producer gas, obtaining minimal variations in these two variables.

In its simplest version, the Rankine cycle consists of four essential components: a pump, a boiler, a steam turbine, and a steam condenser. Due to its nature and parameters, it has relatively low efficiency, and it is possible to expect small capacity systems operating at pressures close to 20 bar and efficiencies in the range of 7–15%, depending on the components' efficiencies included in the cycle and the type of turbine used [20]. An increase in the efficiency of these cycles could be achieved by implementing improvements in the plant's thermal scheme, such as steam reheating and regenerative heating of condensate [21]. All these improvements require a technical-economic analysis to compare the additional investment needed with the profit obtained due to increased efficiency [22]. The

conventional Rankine cycle has been used in several industries, such as sugar, rice, palm oil, paper, and wood to produce electricity, but with relatively low efficiency. However, the low fuel price (waste or biomass from processes), the maturity and reliability of this technology, as well as its relatively low investment cost, make this conversion technology an attractive option [23].

Based on the previous discussion, this paper aims to analyze heavy oil and biomass co-gasification as an alternative for treating these low-values fuels and obtaining co-products such as electricity. For this purpose, a gasification model was developed in Aspen Plus™ software, considering the use of two gasification agents (air and oxygen). Gasification parameters, such as yield, lower heating value (LHV), and composition of producer gas, as well as cold gas efficiency, were evaluated. An analysis of producer gas use in a Rankine cycle was performed using GateCycle™ software, which includes the electricity generation index and boiler performance (boiler efficiency and specific steam production). Furthermore, economic indicators (such as net present value, internal return rate, among others) from the integrated gasification-Rankine cycle system were calculated, aimed at determining the feasibility of the power generation system in the Brazilian context. The economic assessment was developed by using Monte Carlo simulation through Crystal ball™. Thus, this work provides an energy performance and an economic evaluation of the heavy oil and biomass co-gasification process and the potential use of syngas for power generation. It is worth noting that the reviewed literature presents no studies related to energy recovery and its economic assessment from the co-treatment of heavy oil and biomass, which emphasizes the novelty of the current contribution.

## 2. Materials and Methods

### 2.1. Description of Gasification Model

The gasification system was modeled using Aspen Plus™ v.11.0 software, a chemical process modeling, design, and monitoring tool, developed by Aspen Technology, Inc. Since oil heavy oil and biomass are considered non-conventional compounds in the Aspen Plus™ v.11.0, it is necessary to introduce their physicochemical characterization, shown in Tables 1 and 2, respectively, for heavy oil and pruning biomass.

**Table 1.** Heavy oil characterization on dry basis [18,24].

Parameter	Composition (wt.%)
Fixed carbon	67.31%
Volatiles	32.59%
Moisture	0.3%
Ash	0.1%
	Ultimate analysis
Carbon	86.25%
Hydrogen	11.05%
Sulfur	2.2%
Nitrogen	0.4%
Ash	0.1%

**Table 2.** Biomass characterization on dry basis [25].

Parameter	Composition (wt.%)
Volatiles	82.2%
Fixed carbon	15.1%
Moisture	9.0%
Ash	2.7%

Table 2. Cont.

Parameter	Composition (wt.%)
	Ultimate analysis
Carbon	50.5%
Oxygen	40.2%
Hydrogen	6.1%
Ash	2.7%
Nitrogen	0.5%

According to the Brazilian statistical yearbook of oil, natural gas, and biofuels [26], the amount of products obtained through petroleum refining in Brazil (defined as energy derivatives) is approximately 256,700 ton/day, where the heavy oil production corresponded to 38,300 ton/day. Considering that the heavy oil yield is 15% and that all biomass generated in the same refinery is used, a mixture of 50% heavy oil and 50% biomass is considered for this work.

To estimate the variation of the thermodynamic state of the different processes that coexist inside the gasifier, the Peng–Robinson method with Boston–Mathias modifications was used, which is recommended to establish the thermodynamic state of non-polar and medium polar substances. For calculating the thermodynamic properties of the free water phase of the system, the International Association for the Properties of Water and Steam (IAPWS-95) method was implemented [27].

#### 2.1.1. Assumptions Applied to Develop the Gasification Model

The following assumptions were used to develop the gasification model:

- The residence time is long enough to allow the chemical balance to be reached; thus, the gasification process occurs in a steady state regime;
- The reactor is entirely isothermal;
- Chemical reactions are considered time-independent;
- Tar formation is negligible;
- The process is adiabatic;
- The reactor operates at atmospheric pressure;
- Refinery facilities provide electricity auxiliary requirements for gasification;
- Both fuels (heavy oil and biomass) used in gasification are generated at the refinery as residues and, if not used to produce an energy vector (producer gas), may incur costs for their final destination.

Figure 1 shows the flow diagram of the gasification model implemented in Aspen Plus™ software. The fuel flow (FUEL) enters the pyrolysis reactor (PYROL), which simulates the devolatilization of the OILSLU stream through a routine developed in Fortran based on ultimate and proximate analysis of the fuel [28], producing the DEVOL stream, which is composed of volatiles and char. The DEVOL flow goes to the oxidation/combustion reactor (COMBU), which simulates the partial oxidation and char gasification reactions occurring in the process, where the gasification agent (AGENT) is also supplied. The oxidation products (PRODCOMB) are sent to the Gibbs reactor (REDUC), where the reduction reactions occur. Subsequently, PRODRED stream enters the separator SEPAR, which has the function of separating the acid gases, ash, and moisture fractions (RES + MOIS), producing HOTGAS stream, which is cooled down to a temperature of 25 °C to obtain the producer gas stream (SYNGAS). SEPAR considers the method of adsorption using iron oxides, which removes hydrogen sulfide by forming insoluble iron sulfides [29]. The unit operation blocks used in the gasification model are presented in Table 3.

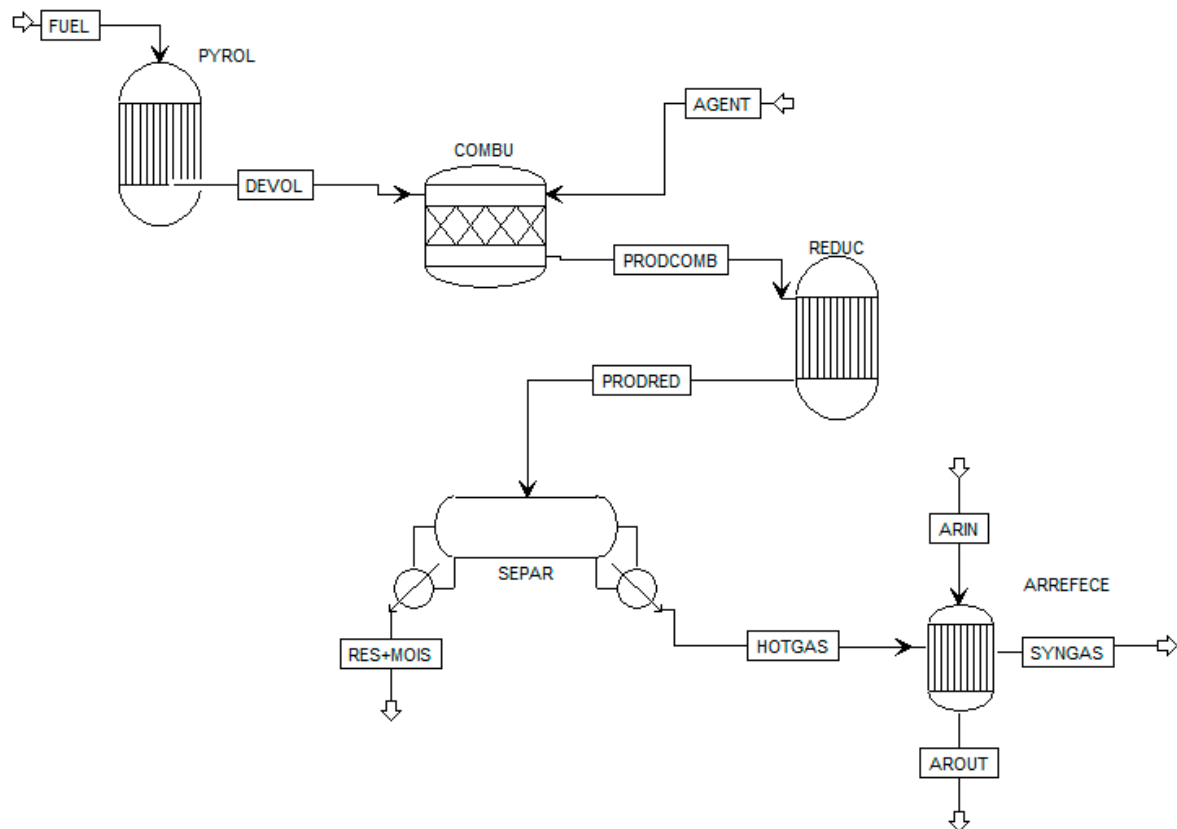


Figure 1. Gasification process.

Table 3. Description of units used in the gasification process.

Block Name	Aspen Plus ID	Description
PYROL	Ryield	Decomposes fuel into conventional components.
COMBU	RStoic	Simulate oxidation reactions of volatiles and char produced in the pyrolysis zone.
REDUC	RGibbs	Simulate reduction reactions considering Gibbs free energy minimization method.
SEPAR	Sep	Separate all contaminants that change the composition of producer gases.
ARREFECE	HeatX	Cool the hot gas to obtain the producer gas.

The computational modeling was developed considering a thermodynamic equilibrium approach, also known as Gibbs's free energy minimization method. In this way, the estimates were based on reaching the thermodynamic equilibrium state, in which the maximum possible energy conversion is obtained [30]. Thus, Equation (1) is used to determine the syngas composition at different operational conditions of the gasification process, considering the number of moles of species present in the system.

$$G^t = \sum_{i=1}^N n_i \Delta \bar{G}_{f,i}^{\circ} + \sum_{i=1}^N n_i RT \ln \left( \frac{n_i}{n_{tot}} \right) \quad (1)$$

where  $\Delta \bar{G}_{f,i}^{\circ}$  corresponds to the standard Gibbs free energy of formation for each species,  $n_i$  is the molar number of each species,  $n_{tot}$  is the total molar amount,  $R$  and  $T$  represent the ideal gas constant and system temperature, respectively.

For a more comprehensive analysis of the thermochemical conversion process, two gasification agents ( $O_2$  and air) are considered. A key parameter for the control and monitoring

of the gasification process is ER, which is defined as the ratio between fuel mass flow and gasification agent at real conditions, divided by the same ratio at stoichiometric conditions:

$$ER = \frac{(\dot{m}_A/\dot{m}_{fuel})}{(\dot{m}_A/\dot{m}_{fuel})_{st}} = \frac{(\dot{m}_{O_2}/\dot{m}_{fuel})}{(\dot{m}_{O_2}/\dot{m}_{fuel})_{st}} \quad (2)$$

where  $\dot{m}_A$ ,  $\dot{m}_{fuel}$ , and  $\dot{m}_{O_2}$  are the mass flow of air, fuel, and O<sub>2</sub>, respectively. The suffix *st* (stoichiometric) represents the amount of air or O<sub>2</sub> required for the complete combustion of fuel.

On the other hand, the performance of a gasifier is measured as a function of syngas quality through the so-called cold gas efficiency (CGE), as shown in Equation (3).

$$CGE = \frac{\dot{Q}_{syngas} \times LHV_{syngas}}{\dot{m}_{fuel} \times LHV_{fuel}} \quad (3)$$

where  $\dot{Q}_{syngas}$  and  $\dot{m}_{fuel}$  are the syngas produced and fuel-fed flows, while *LHV* represents their calorific value.

### 2.1.2. Model Validation

The developed gasification model was validated using the results of Ashizawa et al. [31], who performed Orimulsion™ gasification tests. Table 4 presents the gasifier operating conditions and the feedstock characterization used for model verification.

**Table 4.** Fuel characterization and operational parameters for model verification [31].

Operational Parameter	Value
Pressure	18.75 atm
Gasification agent	Oxygen
Equivalence ratio	0.4
Ultimate analysis (wt.% on dry basis)	
Carbon	84.28%
Hydrogen	10.33%
Sulfur	3.95%
Nitrogen	0.64%
Oxygen	0.55%
Ash	0.25%
Proximate analysis (wt.% on dry basis)	
Volatiles	81.71%
Moisture	28.80%
Fixed carbon	18.04%
Ash	0.25%

Table 5 shows a comparison of the results generated by the computational model developed in this study and the work of Ashizawa et al. [31]. The results do not show significant differences between the volumetric fractions of the producer gas obtained with the presented model and those obtained by Ashizawa et al. [31], resulting in an RMS error of 0.02, which can be considered a suitable value for a computational model of gasification processes.

**Table 5.** Comparison between the results obtained in the model and the experimental work.

Parameter	Ashizawa et al. [31]	This Work
CO	38.70%	40.69%
H <sub>2</sub>	39.40%	35.73%

Table 5. Cont.

Parameter	Ashizawa et al. [31]	This Work
H <sub>2</sub> O	11.85%	14.45%
CO <sub>2</sub>	8.67%	8.01%
Other	1.30%	1.02%
CH <sub>4</sub>	0.08%	0.10%
H <sub>2</sub> /CO ratio	1.02	0.88
RMS	-	0.02

## 2.2. Rankine Cycle

The conventional Rankine cycle scheme developed in the GateCycle™ software is shown in Figure 2. Stream 1 represents the producer gas from the gasification process. The superheated steam (2) is expanded in the steam turbine, generating shaft work, while the low-pressure steam flow (3) is sent to the condenser. The condensed water (7) is pressurized in the pump (8) and then sent back to the boiler, passing through a deaerator, closing the cycle.

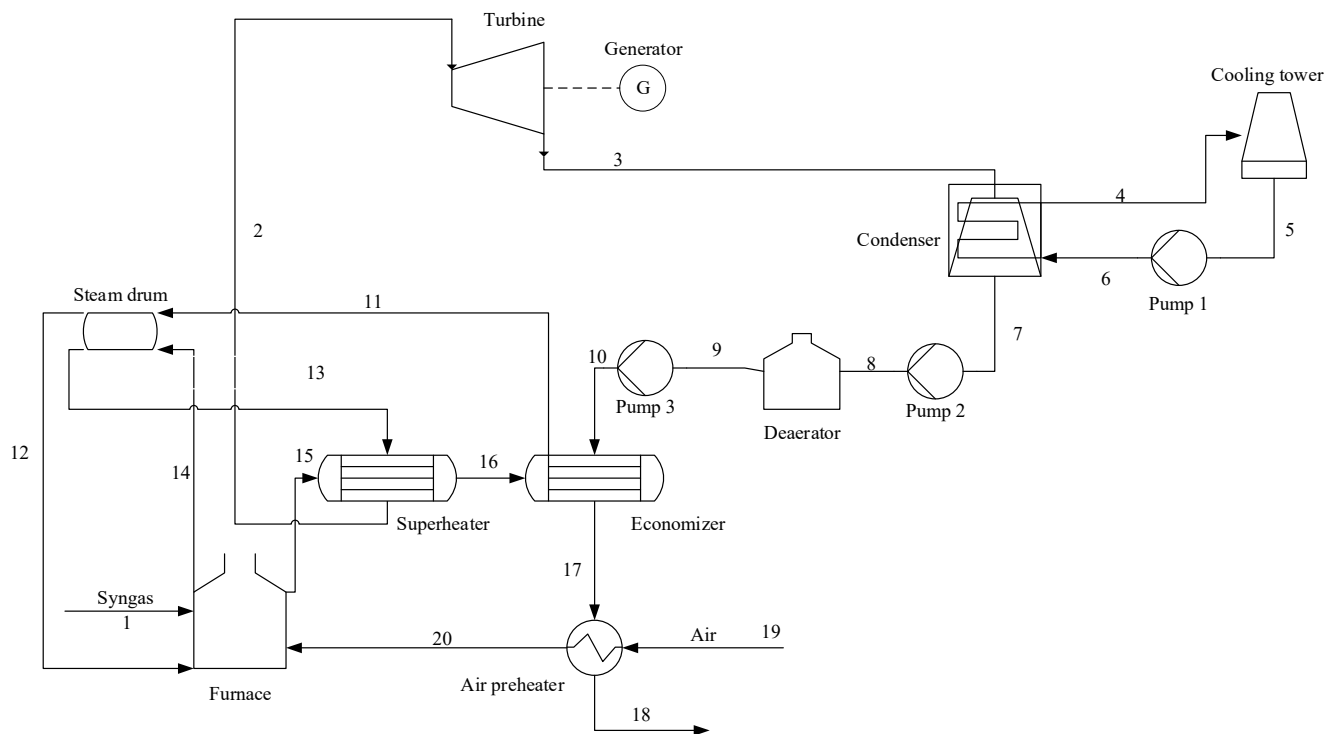


Figure 2. Rankine cycle schematic.

For Rankine cycle simulations, it was considered the average annual climatological data for Belo Horizonte city (where the biomass and heavy oil originated/crude refinery location). Therefore, as reported by the Brazilian National Institute for Meteorology (INMET), a temperature of 22 °C, pressure of 101.9 kPa, and relative humidity of 67.2% were used. Some of the considerations adopted for model development are as follows:

- Steady-state process;
- It used a condensing turbine;
- The heat rejection of the steam cycle occurred through a water-cooled condenser and a wet cooling tower;
- Steam boiler was modeled considering its components (steam drum, furnace, superheater, economizer, air preheater), where the main input parameters that were considered, are presented in Table S1 of Supplementary Material.



The operating parameters of the Rankine cycle components are presented in Table 6, while the complete scheme of the power plant is shown in Figure S1 of Supplementary Material.

**Table 6.** Rankine cycle parameters [32–34].

Steam Turbine		Steam Boiler	
Type	Condensation	Steam temperature	360 °C
Live steam temperature	350 °C	Steam pressure	23 bar (g)
Shaft power	300 kW	<b>Condenser</b>	
Isentropic efficiency	60%		
Live steam pressure	23 bar (g)	Maximum cooling water temperature	32 °C
Exhaust pressure	0.12 bar (g)	<b>Pump</b>	
<b>Generator</b>			
Efficiency	96%	Rotation	3600 rpm
Power factor	0.8	Isentropic efficiency	70%

### 2.3. Economic Assessment

The economic feasibility of the system was determined following the steps described in Figure 3, which represents a test model for power generation projects complemented with risk analysis. The used currency was the United States Dollar (USD) of July 2022.

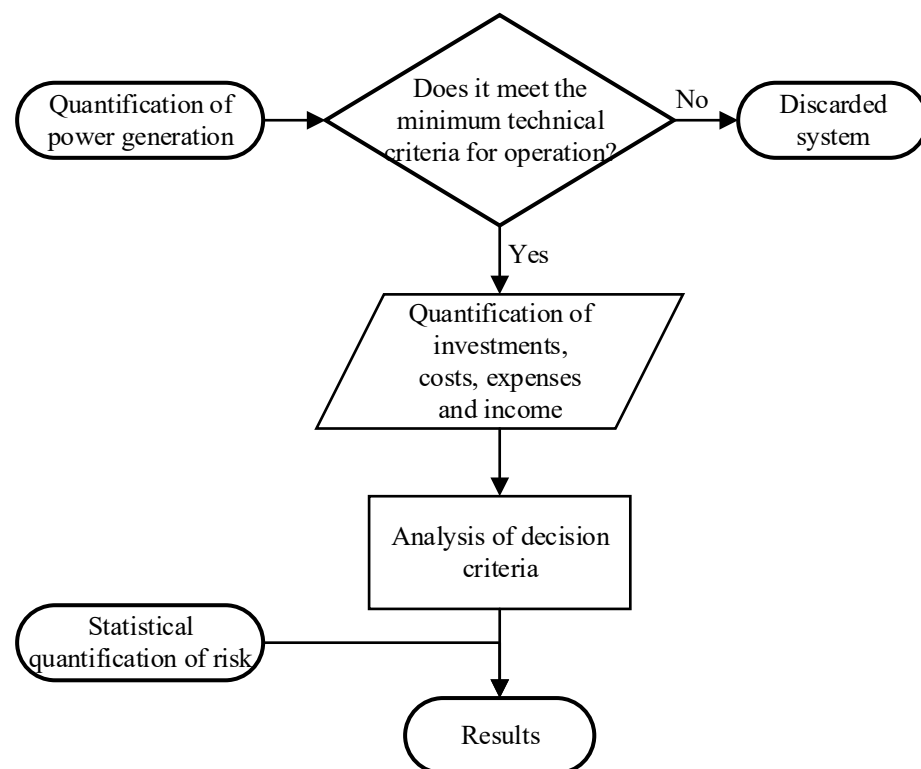


**Figure 3.** Stages of the economic feasibility study of the system.

Once it was established that the produced syngas has a suitable energy density to drive steam power generation systems (syngas LHV was higher than 3.0 MJ/Nm<sup>3</sup>) [35], the system's operational expenditures, revenues, and capital expenditures were calculated. The costs of the power cycle, gasifier, oxygen supply unit, and import duties were determined based on literature consultations [36–38].

The risk analysis was developed in Crystal Ball<sup>®</sup> v11.1.2.4.850, a computational tool developed by Oracle Corporation<sup>™</sup> (Austin, TX, USA) that enables the modeling, forecast-



ing, and optimization of scenarios containing any uncertainty through stochastic Monte Carlo simulations. The adopted assumptions (variables with some degree of uncertainty) considered during the risk study were:

- Power delivered by the system,
- Gasifier operating and maintenance costs,
- Power cycle operating and maintenance costs,
- Local electricity tariff,
- United States Dollar and Brazilian Real exchange rate,
- Oxygen price (only in the scenario that uses oxygen as a gasification agent).

Operating and maintenance costs for gasification systems (not including the fuels) range from 3.5% to 5.7% of their capital expenditure (CAPEX), according to [15]. In this study, the mean value of the range (4.60%) was taken as a starting parameter. The risk study incorporated the lower and upper limits through a triangular distribution. Operating costs for the power cycle were estimated at 1.9 ¢/kWh from [39], with lower and upper limits of 1.8 ¢/kWh and 2.0 ¢/kWh during risk analysis, respectively.

Revenues (savings due to own electricity generation) were projected based on the electricity tariff currently applied by a local utility company, considering the history of increases in recent years and the forecasts for coming years. Before taxes, the base case's reference value for the electricity tariff was 0.1614 USD/kWh.

Considering that heavy oil is a low value-added fuel produced in the refinery, its price could be established as that of fuel for the conventional steam power plant; thus, this cost is 170 USD/ton, adjusting (between July 2016 and August 2022) the suggested price by Reyhani et al. [40]. Regarding biomass pruning, it is worth noting that these must be pretreated, stored, and transported before their use as fuel. Therefore, the biomass cost is 95 USD/ton, adjusting (between February 2019 and August 2022) the value indicated by Sagani et al. [41]. Adjustments were made based on the Brazilian producer price index [42]. On the other hand, the dollar exchange rate variation was determined from the statistical adjustment of the history of the last twelve months, according to data published by the Central Bank of Brazil [43]. The reference value for the dollar exchange rate used during the economic assessments was 5.03 BRL/USD.

The minimum attractive rate of return (MARR) was linked to the weighted average cost of capital (WACC) of a renewable energy company with a capital structure of 60% equity and 40% third-party debt. The WACC was determined using the Capital Asset Pricing Model (CAPM). The cost of equity ( $R_E$ ) was determined using Equation (4) from the energy sector factor ( $\beta$ ), the risk-free rate ( $R_F$ ) and the expected return of the market ( $R_M$ ) [44].

$$R_E = R_F + \beta(R_M - R_F) \quad (4)$$

where  $R_F = 4.5\%$  APR (annual percentage rate);  $R_M = 13.00\%$  APR (expected rate for productive projects); and  $\beta = 0.4517$ ; therefore  $R_E = 8.34\%$  APR. Note that in this case, the spread is 8.50% APR. Considering  $R_E$ , the WACC of the enterprise was estimated through Equation (5) using a financing rate ( $R_D$ ) of 13.28% APR.

$$WACC = R_D \times D \times (1 - T) + R_E \times E \quad (5)$$

where  $D = 0.40$  (market value of debt);  $E = 0.60$  (market value of equity);  $R_D = 13.28\%$  APR;  $R_E = 8.34\%$  APR; and  $T = 0\%$  (corporate tax rate) as the savings resulting from the implementation of the proposed system are exempt from taxation. Therefore,  $WACC = 10.32\%$  APR.

With the probability distributions, the risk of the project becoming unfeasible was quantified from a Monte Carlo simulation with 30,000 trials and a confidence level of 95%, considering the lower permissible limits of the economic decision criteria, which are net present value (NPV) > USD 0.00 and MARR > 10.32% APR. Other relevant factors during the economic feasibility analysis for the power system based on air as the gasification agent are described in Table 7.

**Table 7.** Complementary data for the economic feasibility study of the power system.

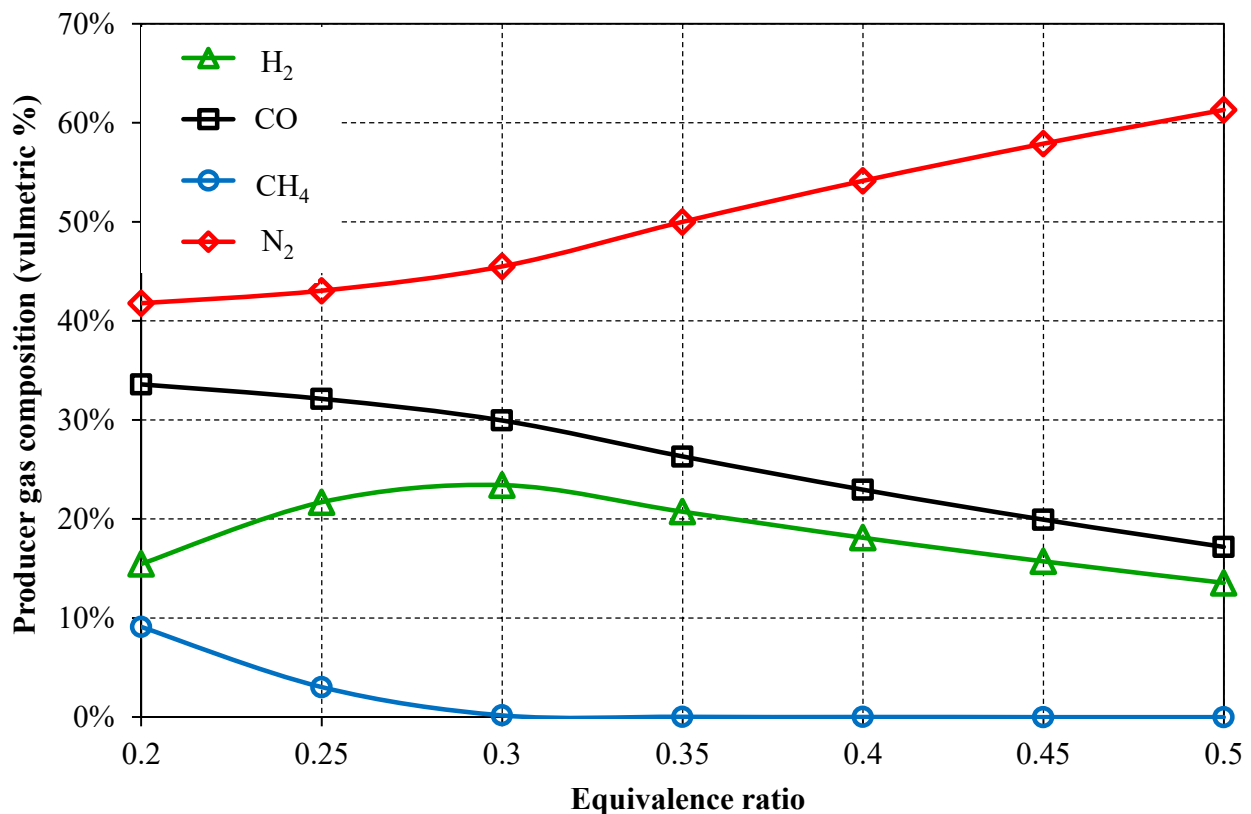
Factor	Unit	Value	Reference
System service life	Year	15	-
BRL to USD Exchange	BRL/USD	4.92–5.79	[43]
Depreciation	% APR	10.00	[45]
MARR (WAAC)	% APR	10.32	-

The input parameters with probability distribution considered for annual revenue and expenses of the power generation system are described in Table S2 of the Supplementary Material.

### 3. Results and Discussion

#### 3.1. Producer Gas Composition

The producer gas obtained from the co-gasification process using air as a gasification agent reach a significant content of  $H_2$  (23.7% for  $ER = 0.3$ ) and other compounds such as  $CO$  and  $CH_4$ , which contribute to the increase of producer gas LHV. Thus, Figure 4 shows the expected composition profile in the producer gas obtained after co-gasification as a function of ER. In general, it was observed that the increase in ER favors the thermal cracking and reforming steam reactions, reducing the concentration of  $CH_4$  (varying from 9.1% to 3.0%), although a higher concentration of  $H_2$  and  $CO$  were obtained in the same ER range (between 0.2 and 0.3) [46].

**Figure 4.** Effect of ER on the composition for air gasification.

On the other hand, it can be seen that the nitrogen content in the producer gas is quite expressive and increases rapidly, from 41.8% to 61.3%, with the increase of ER (from 0.2 to 0.5) associated with the greater amount of air supplied in the system. From Figure 5, one can observe that when oxygen is provided as the gasification agent, there are higher

fractions of CO (33.6% as a maximum value) and H<sub>2</sub> (57.6% as a maximum value) for the ER range between 0.2 and 0.5 due to the nitrogen absence. A similar behavior (based on Figure 4) is obtained for the CH<sub>4</sub> fraction because this chemical compound decreases from 15.9% to 0.1% for the studied ER range.

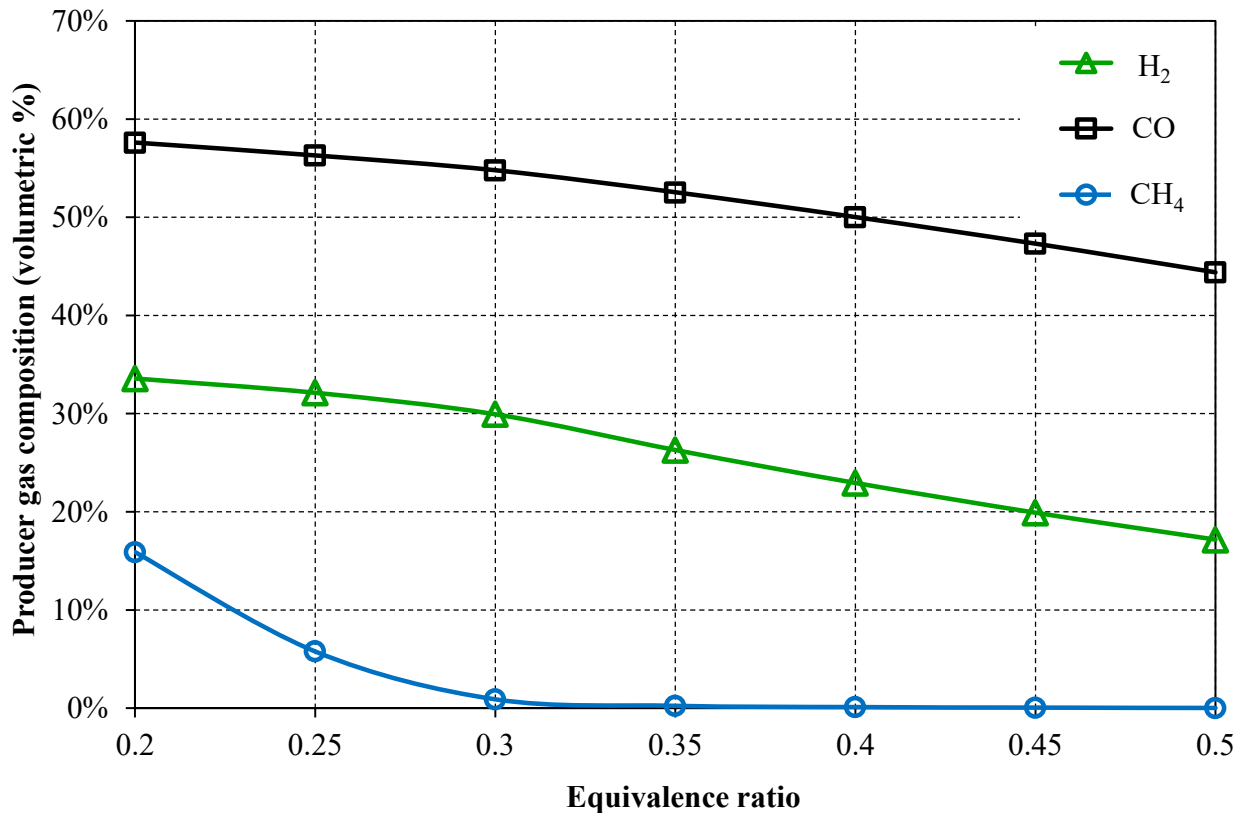


**Figure 5.** Effect of ER on the composition for oxygen gasification.

### 3.2. Producer Gas LHV

Regarding producer gas LHV, a decreasing trend was observed as ER increased until reaching values that oscillate in the range of 6.37 and 3.63 MJ/Nm<sup>3</sup> for ER values greater than 0.30 when using air as the gasification agent (see Figure 6). This behavior is associated with a higher amount of gasification agent supplied, which favors the reforming and thermal cracking reactions of the heavier organic fractions contained in heavy oil. Thus, lighter hydrocarbons are produced with lower energy content, leading to a mixture of lighter combustible gases and consequently decreasing the LHV [47]. Otherwise, the oxygen co-gasification case presented better results of LHV, decreasing from 11.79 to 9.40 MJ/Nm<sup>3</sup> (for ER greater than 0.3), associated with higher concentrations of H<sub>2</sub>, CO, and CH<sub>4</sub>.

### 3.3. Producer Gas Yield

Another critical parameter in gasification is related to the producer gas yield, which has an increasing trend as the ER values increase, as shown in Figure 7 and reported by Upadhyay et al. [48] and Pandey et al. [49]. Considering an ER of 0.30 for the air co-gasification case, the producer gas yield is expected to be around 4.48 Nm<sup>3</sup>/kg fuel. However, as the amount of gasification agent injected into the reactor increases, the decomposition and reformation of heavier hydrocarbons are favored, and consequently, a greater amount of gas per unit of fuel mass is generated [50]. For the oxygen co-gasification case, there exists an inverse relationship between producer gas LHV and the yield since greater values of the LHV lead to a smaller volume produced of gas per unit of dry fuel fed due to the partial removal of nitrogen from the provided gasification agent.

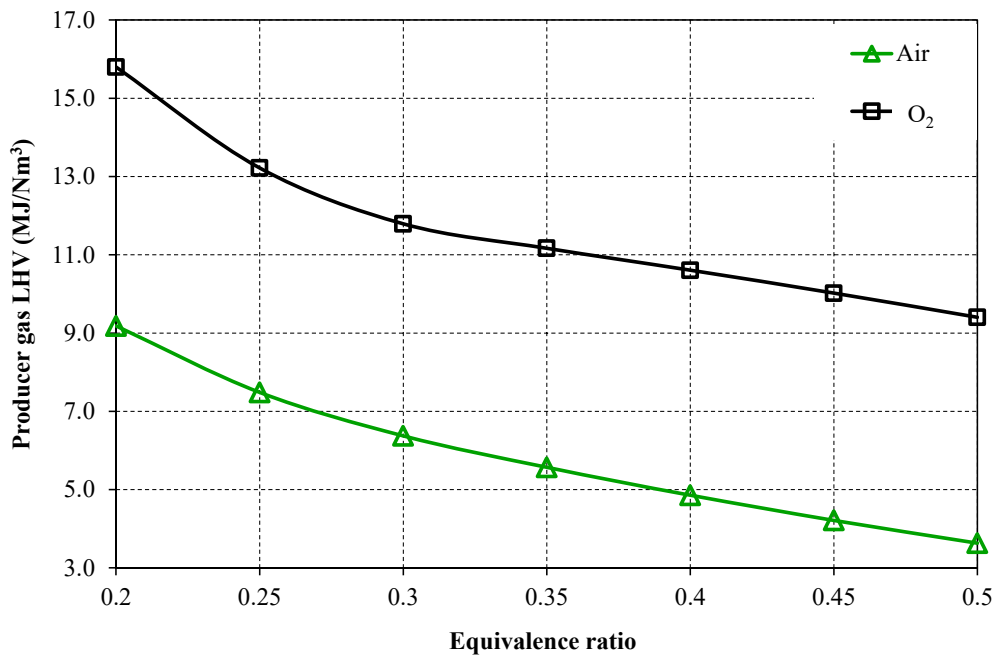


Figure 6. Producer gas LHV.

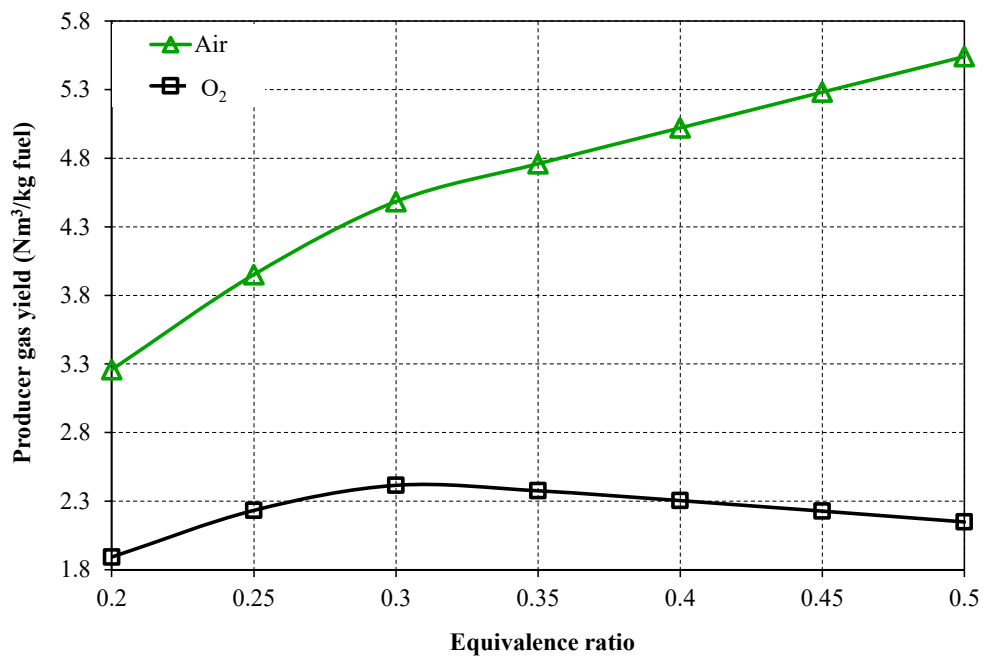


Figure 7. Producer gas yield.

### 3.4. Cold Gas Efficiency

The cold gas efficiency (CGE) of the gasification process is calculated considering the values obtained from the LHV and producer gas yield, as presented in Figure 8. As can be seen, for the analyzed ER range, the CGE of the co-gasification process decreases from approximately 91% to 61%, for both cases. This behavior occurs because a greater supply of oxidant (air or O<sub>2</sub>) favors the production of CO<sub>2</sub>, leading to a decrease in the composition of combustible gases in the producer gas. The reduction is slightly higher for air co-gasification due to the N<sub>2</sub> present in the air, which will also be part of the producer gas composition as it is a chemically inert compound [51].

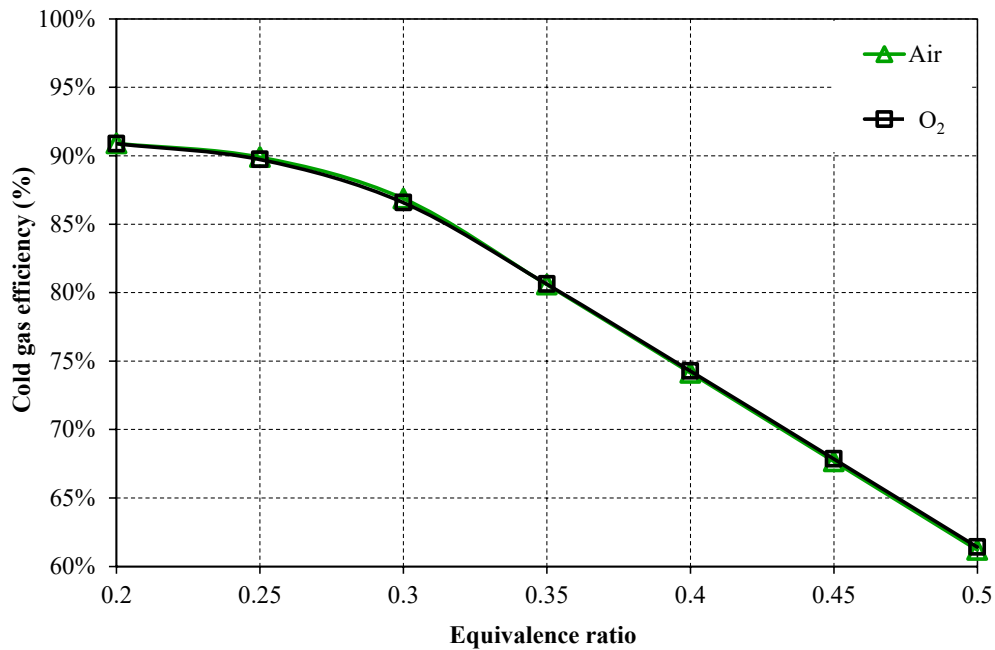


Figure 8. Cold gas efficiency.

### 3.5. Producer Gas Specific Energy

Producer gas specific energy (Figure 9) considers the chemical energy and the sensible heat associated with the gas mass flow at the gasifier outlet. Usually, producer gas is cooled down before being fed to drive the Rankine cycle, and its sensible heat is not considered. Thus, in this work, chemical energy recovery from producer gas is contemplated as a strategy for evaluating the electricity generation index of the process.

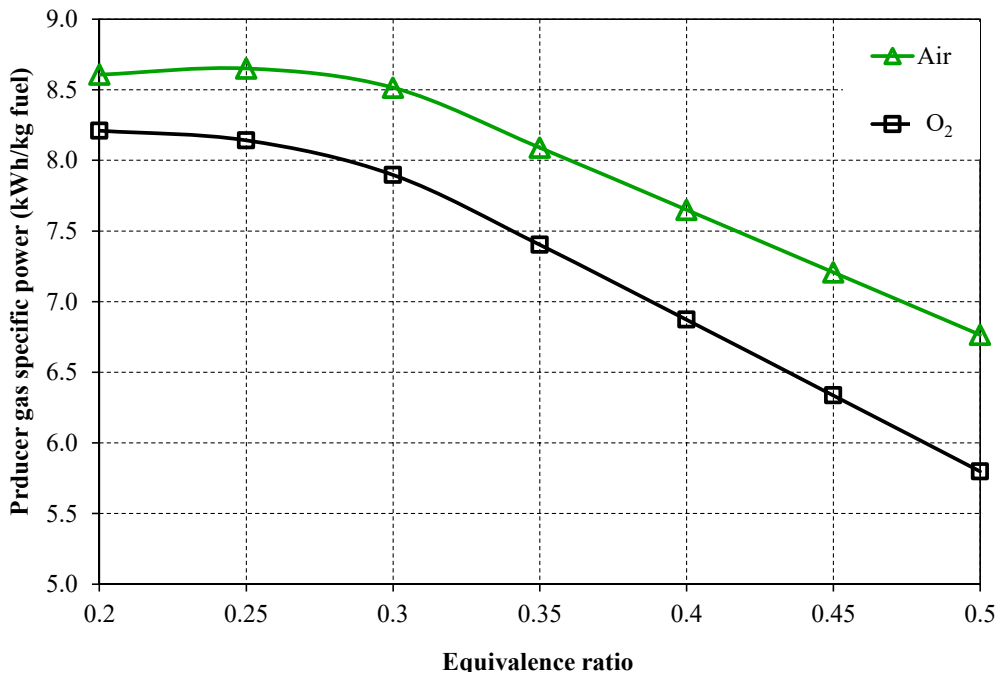


Figure 9. Producer gas specific power.

Producer gas specific energy tends to decrease for higher ER values when using oxygen as a gasification agent, reaching values close to 7.9 kWh/kg fuel at ER 0.3, while for air

co-gasification, it was 8.5 kWh/kg fuel. This decreasing tendency could be associated to the presence of  $N_2$  and steam, which encourages the dilution effect and steam reforming of  $CH_4$ , respectively, thus deteriorating the producer gas quality in terms of specific energy [52].

### 3.6. Electricity Generation Obtained from Rankine Cycle

The analysis of the Rankine cycle is based on the parameters presented in Table 6, where the isentropic turbine efficiency, the condensate pressure, and the isentropic pump efficiencies, as well as the pressure and temperature conditions of superheated steam entering the turbine are fixed. The ER values considered in the Rankine cycle analysis (Figures 10 and 11) refer to the conditions in which the producer gas is obtained in the gasification process, considering a fuel flow (50% of heavy oil and 50% of biomass) of 200 kg/h, as suggested by Zoungrana et al. [53] for fixed-bed gasifiers.

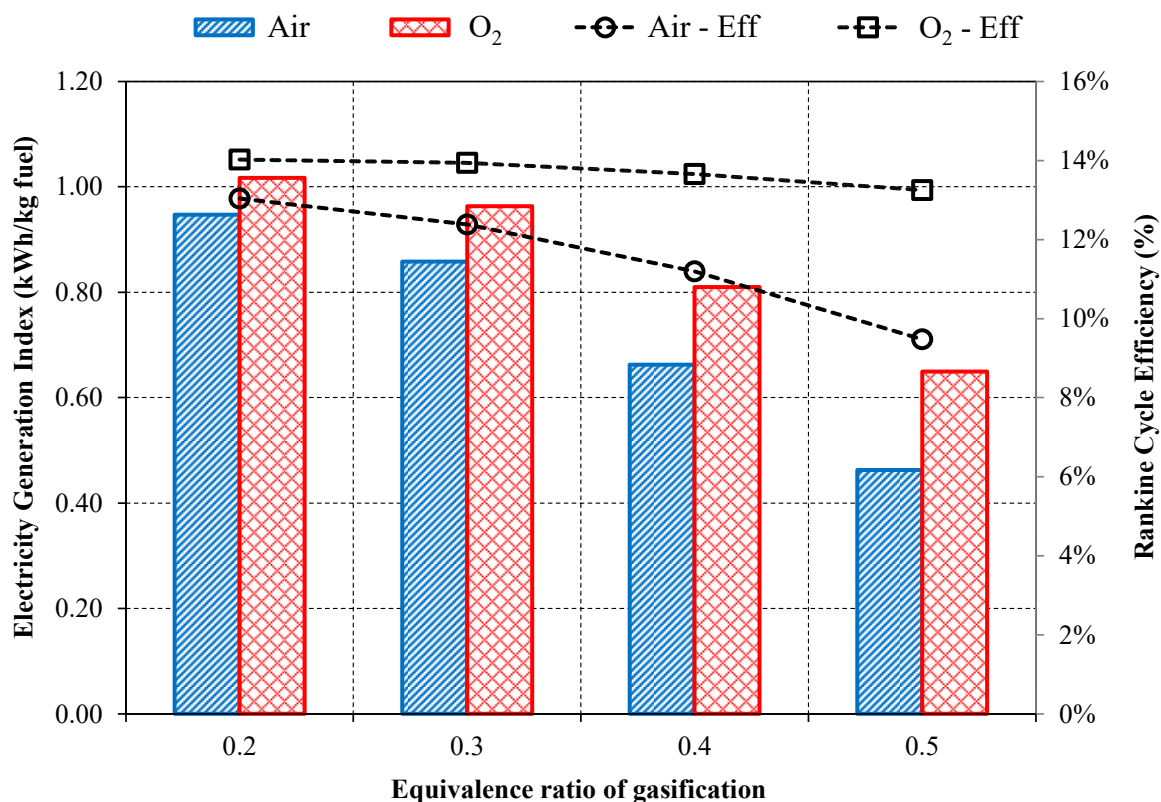
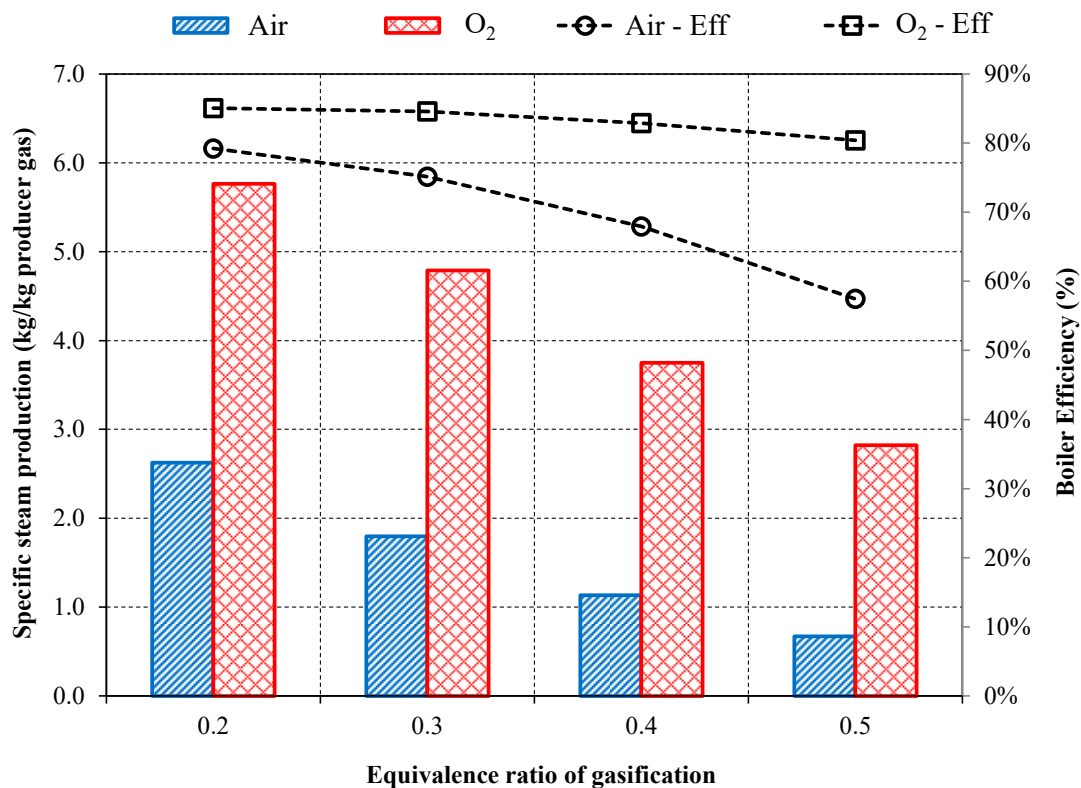


Figure 10. Electricity generation index from producer gas use in Rankine cycle.

Figure 10 shows the electricity generation index obtained in the Rankine cycle using the producer obtained in both co-gasification cases. As can be observed, for oxygen co-gasification, higher electricity generation indexes (1.02–0.65 kWh/kg fuel) are obtained compared to those obtained for air gasification (0.95–0.46 kWh/kg fuel) in ER range studied. This occurs because the producer gases from oxygen gasification have higher values of LHV (Figure 6) and, therefore, higher chemical energy [54].

In addition, Figure 10 indicates that greater electricity generation is related to greater cycle efficiencies, which is mainly affected by boiler efficiencies (designed to operate at different conditions). It is worth noting that the values of enthalpy for the water entering and steam leaving the boiler are constant; therefore, the boiler efficiency is influenced by the steam flow generated and LHV of syngas, as indicated by the direct method. For air co-gasification, the obtained Rankine cycle efficiency range lies between 13.0% and 9.5%, and for oxygen co-gasification, from 14.0% to 13.2%, which also shows the influence of producer gas composition (Figures 4 and 5); as mentioned, producer gases from oxygen

co-gasification have higher values of LHV when compared to gases from air co-gasification, associated to higher energy density [55].



**Figure 11.** Energy performance indicators of Rankine cycle boiler.

Regarding boiler efficiency, it is worth noting that the gases obtained from co-gasification using air as the gasification agent present significant reductions in the LHV (9.62 to 3.63 MJ/Nm<sup>3</sup>) as a function of ER. Thus, boilers were adapted for the chemical energies associated with each of the obtained gases, resulting in a significant reduction in boiler efficiency, from 79.2% to 57.5%, while for the gases produced in co-gasification with oxygen as the gasification agent, for which the LHV were higher (15.8 to 9.4 MJ/Nm<sup>3</sup>), the boiler efficiency was reduced from 85.1% to 80.4%, as shown in Figure 11. These efficiencies are in agreement with the ones obtained for boilers with similar capacity and operating conditions [56]. On the other hand, as the effectiveness of the air preheater is held constant, there is a reduction in the energy recovered from the exhaust gases to preheat the air, and the boiler exhaust temperature (exit of the air preheater) tends to increase [57].

Figure 11 also shows that the decrease in boiler efficiency leads to a decline in specific steam production. For air co-gasification, the variation is from 2.6 to 0.7 kg/kg-producer gas, while for oxygen co-gasification, it is from 5.8 to 2.8 kg/kg-producer gas. The main effect of this reduction is the reduction in electrical energy generation because as less steam is fed to the turbine, less power is produced [58].

### 3.7. Economic Analysis

The main technical and economic characteristics of the power system based on air and oxygen as gasification agents are described in Table 8. Since the equipment required to build the system is not available in the domestic market, it will be necessary to pay the taxes shown in Table 9 for importing them.



**Table 8.** Investment required to build the power system.

Feature or Item	Unit	Air Operation	Oxygen Operation
Active power	kW	92.53–189.39	129.9–203.4
Availability	%	95.00	95.00
Annual energy generated	kWh/year	770,094–1,576,071	1,081,051–1,692,861
<b>Investment</b>			
Power cycle	USD	268,381	268,381
Gasifier	USD	310,274	310,274
Balance of plant—BOP [59]	USD	115,731	115,731
Taxes	USD	59,101	59,101
<b>Total</b>	<b>USD</b>	<b>753,487</b>	<b>753,487</b>

**Table 9.** Taxes arising from the import of equipment to Brazil.

Tax	Value	Ref.
TEC Mercosur—Common External Tariff	0.00%	[60]
IPI—Tax on Industrialized Products	8.00%	[61]
PIS—Social Integration Program	2.10%	[62]
COFINS—Contribution to Social Security Financing	9.65%	[62]
ICMS—Tax on Movement of Goods and Services	18.00%	[63]
<b>Total</b>	<b>37.75%</b>	

The annual revenues, the product of savings in terms of electricity not consumed from the electrical grid (avoided cost), are described in Table 10. On the other hand, the annual operating and maintenance expenses for the power system are presented in Table 11.

**Table 10.** Annual revenue from the power system.

Parameter	Unit	Air Operation	Oxygen Operation
Electricity rate (before taxes)	BRL/kWh	0.53–1.54	0.53–1.54
Electricity generation rate (before taxes)	BRL/kWh	1.53–3.45	4.82–10.89
BRL to USD Exchange	BRL/USD	4.92–5.79	4.92–5.79
Electricity taxes (B3 class)	%	25.00	25.00
<b>Annual revenue</b>	<b>BRL/year</b>	<b>2,981,217</b>	<b>3,200,123</b>

**Table 11.** Annual expenses of the power system.

Annual Expenses	Unit	Air Operation	Oxygen Operation
Gasifier operating and maintenance cost	USD	12,072	15,213
Power cycle operating and maintenance cost	USD	27,406	32,390
Oxygen	USD	0.00	333,688
Heavy oil and biomass cost *	USD	441,066	441,066
<b>Total</b>	<b>USD</b>	<b>480,544</b>	<b>822,356</b>

\* Heavy oil cost as fuel for the conventional steam power plant.

From the data (discount rate, segregation of investment, and segregation of expenses) and with the estimate of the annual savings resulting from the implementation of the power system based on air as gasification agent; it is possible to obtain the probability distribution of the NPV and shown in Figure 12. Note that the host company's initial investment would be USD 753,487. Considering the behavior of the NPV, the investment is economically unfeasible. The loss probability corresponds to 62.41% for the internal return rate (IRR) and 92.09% for NPV.

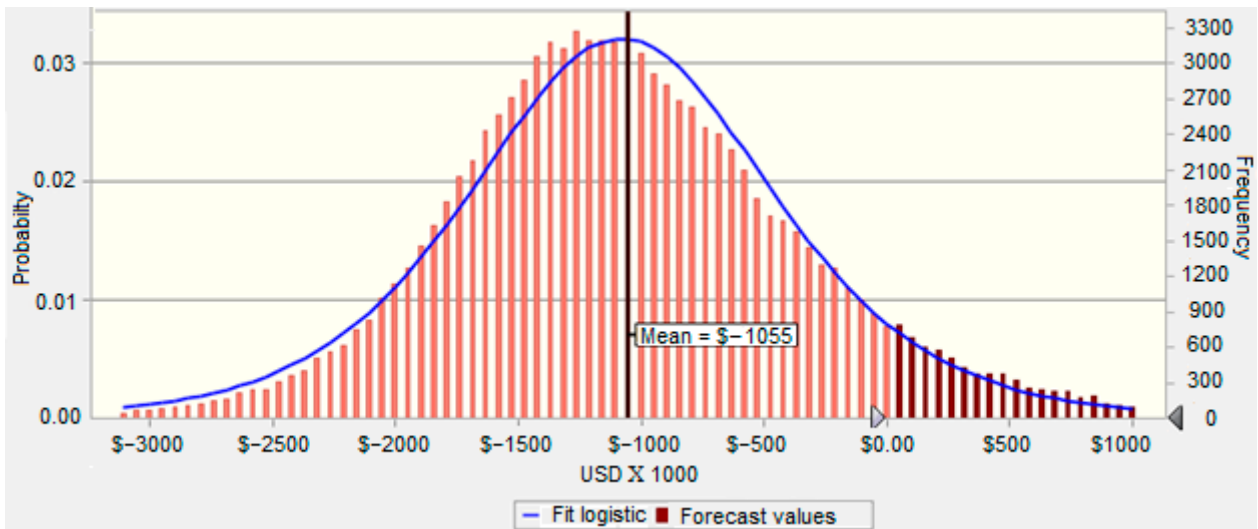


**Figure 12.** Prediction of NPV behavior for power system based on air as a gasification agent.

As shown in Figure 13, the project’s NPV highly depends on the electricity rate and the delivered net electric power. The BRL to USD exchange rate and the operation and maintenance costs have a negligible effect on the system’s economic viability. Therefore, the Rankine cycle/gasifier system using air as a gasification agent will be viable if the electricity tariff is at least 1.68 BRL/kWh.

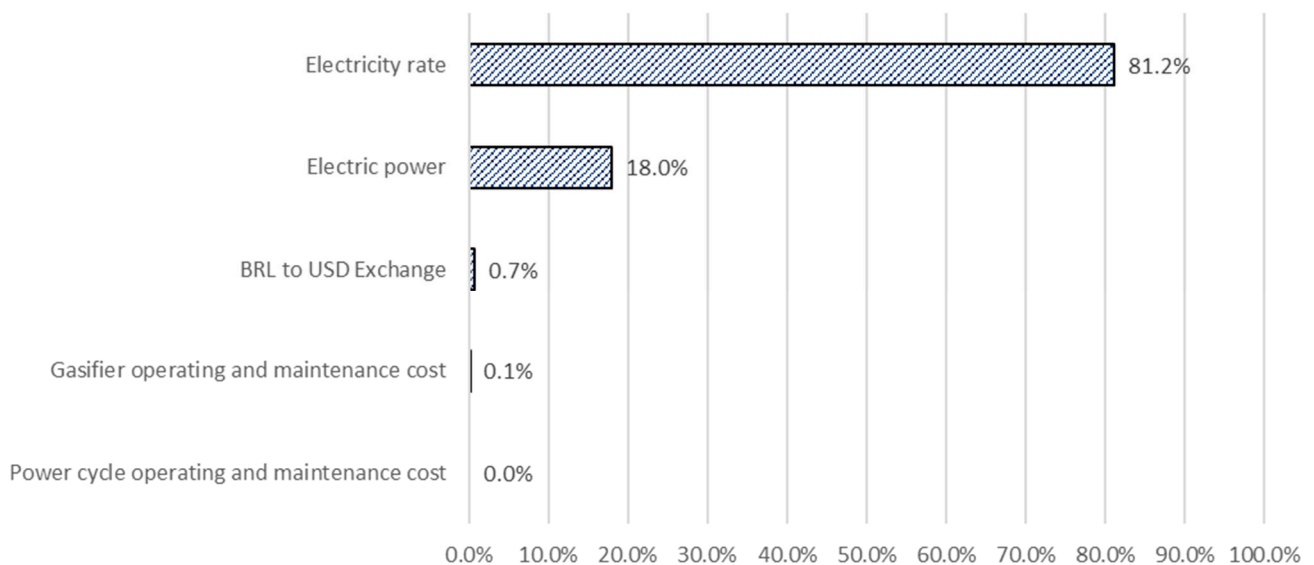


**Figure 13.** Assumption contribution to NPV variance of power system based on air as a gasification agent.

Based on the discount rate, investment and expenses value segregation, as well as on the estimate of the annual savings resulting from the implementation of the system that uses oxygen, the probability distribution of the NPV is calculated (Figure 14). It could be observed that the host company’s initial investment would be USD 753,487, the same as the power system based on air as a gasification agent (Table 7).

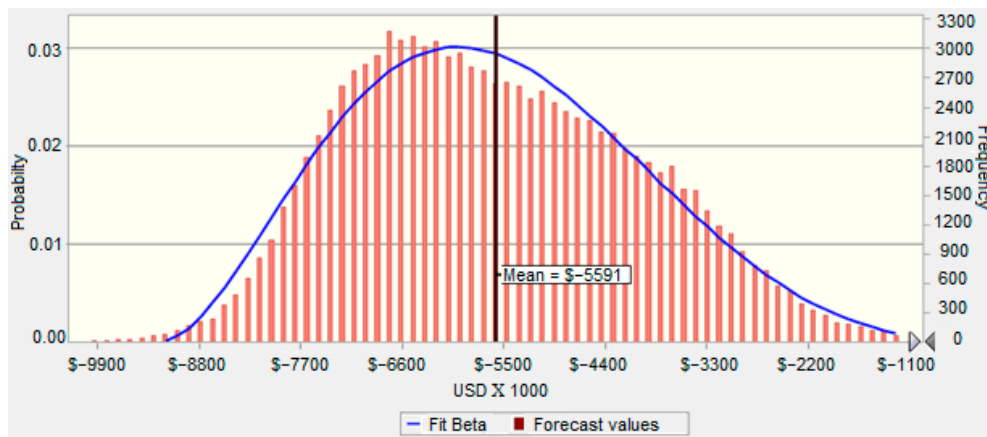


**Figure 14.** Prediction of NPV behavior for power system based on oxygen as a gasification agent.

From the results obtained for NPV, it can be concluded that the investment is economically unfeasible. The probability of having a loss (negative NPV or IRR lower than MARR) corresponds to 65.51% (for IRR) and 99.70% (for NPV).

Like the system that uses air, Figure 15 shows that the project's NPV is dependent on the electricity rate and the net electric power delivered, while the BRL to the USD exchange rate as well as the operation and maintenance costs had a minimal effect on the economic viability of the system. Therefore, the Rankine cycle/gasifier system using oxygen as a gasification agent will be viable if the electricity tariff is at least 4.40 BRL/kWh.

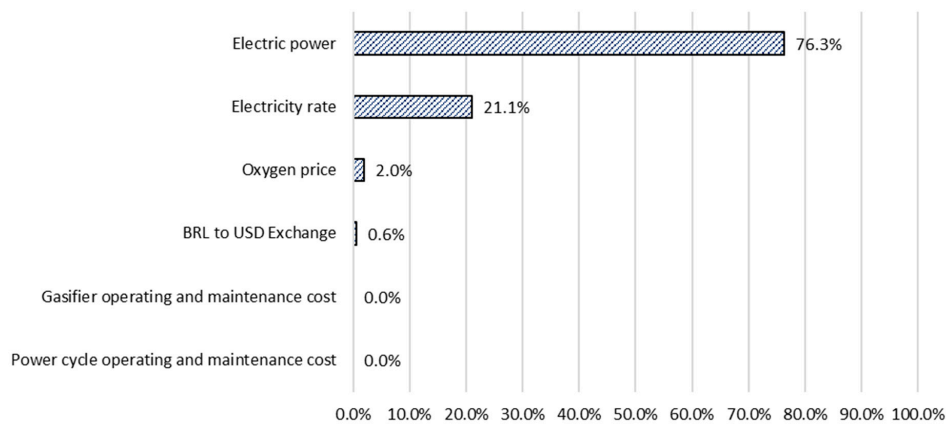


**Figure 15.** Assumption contribution to NPV variance of power system based on air as a gasification agent.

#### 4. Conclusions

An energetic and economic assessment of electricity generation through a gasification system coupled to a Rankine cycle was carried out, considering that the gasifier was fed with heavy oil and biomass in a proportion of 50%/50%, using air and oxygen as gasifying agents. The results indicated that the use of air as a gasifying agent leads to a decrease in the syngas LHV (from 6.37 and 3.63 MJ/Nm<sup>3</sup>) as the ER increases from 0.3 to 0.5 and a volumetric concentration of H<sub>2</sub> (23.7%) for ER = 0.3, while a reduction in methane concentration (from 9.1% to 3.0%) was observed. In the oxygen co-gasification scenario, increasing trends were obtained for CO and H<sub>2</sub> fractions as the ER rose from 0.2 to 0.5, while the syngas LHV decreased from 11.79 to 9.40 MJ/Nm<sup>3</sup> as the ER increased from 0.3 to 0.5.

The syngas yield corresponded to 4.48 Nm<sup>3</sup>/kg-fuel when the air was used (ER = 0.3); thus, it could be appropriate to mention that the syngas yield increased due to the cracking

of heavy chemical compounds present in the fuel mixture composition. For co-gasification with oxygen, an inversely proportional relationship was observed between the LHV and the yield of the syngas, in this case, as the LHV increases (0.3 to 0.5 MJ/Nm<sup>3</sup>), the amount of gas produced decreases (2.4 to 2.2 Nm<sup>3</sup>/kg). On the other hand, co-gasification with oxygen presented a higher electricity production rate (1.02–0.65 kWh/kg fuel) compared to co-gasification with air (0.95–0.46 kWh/kg fuel) because the syngas produced with oxygen has higher chemical energy associated with LHV.

An economic evaluation was performed for the analyzed systems, considering the nominal electrical power and the local electricity tariff, where operation and maintenance costs have a secondary role in the evaluation. Besides, the results showed that the amount of energy the air-based and oxygen-based power systems generates is insufficient to guarantee a return on investment. The critical factors within the economic study of both system variants are the rated electrical power and the local electricity rate. The currency exchange rate and the operation and maintenance (O&M) costs play a secondary role in economic assessment.

With reliability of 95%, it is possible to state that the power system based on oxygen as a gasification agent has a probability of up to 99.7% generating economic losses, whereas for air-based power system corresponds to 92.09%. Therefore, it is essential to analyze the technologies and gasifying agents before implementing gasification/power systems.

**Supplementary Materials:** The following supporting information can be downloaded at: <https://www.mdpi.com/article/10.3390/pr10112358/s1>, Figure S1: Power Plant Scheme; Table S1: Input parameters for the modeling of boiler component; Table S2: Input parameters for economic assessment.

**Author Contributions:** Conceptualization, N.C.H. and Y.C.S.; methodology, O.J.V. and Y.C.S.; software, N.C.H. and Y.C.S.; validation, Y.C.S. and N.C.H.; formal analysis, L.A.S. and O.J.V.; investigation, T.T.G.d.R. and L.A.S.; resources, S.V.D. and T.T.G.d.R.; data curation, G.V.O. and L.A.S.; writing—original draft preparation, N.C.H. and Y.C.S.; writing—review and editing, O.J.V. and S.V.D.; visualization, S.V.D.; supervision, T.T.G.d.R.; project administration, G.V.O.; funding acquisition, L.A.S. and O.J.V. All authors have read and agreed to the published version of the manuscript.

**Funding:** The authors would like to acknowledge the financial support from the Coordination for the Improvement of Higher Education Personnel (CAPES), Brazilian Council for Scientific and Technological Development (CNPq), the PRH of the National Agency for Petroleum, Natural Gas, and Biofuels (PRH-ANP n°51.1), and Carlos Chagas Filho Foundation for Research Support in the State of Rio de Janeiro (FAPERJ).

**Data Availability Statement:** Not applicable.

**Conflicts of Interest:** The authors declare no conflict of interest.

## Nomenclature

APR	Annual percentage rate
CGE	Cold gas efficiency
ER	Equivalence ratio
IRR	Internal return rate
LHV	Lower heating value
MARR	Minimum attractive rate of return
NPV	Net present value
WACC	Weighted average cost of capital
$\dot{m}$	Mass Flow (kg/h)
$D$	Market value of debt (-)
$E$	Market value of equity (-)
$R_D$	Financing rate (%)
$R_E$	Cost of equity (%)
$R_F$	Risk-free rate (%)
$R_M$	Expected return of the market (%)
$T$	Corporate tax rate (%)

## References

1. Organization of the Petroleum Exporting Countries. *World Oil Outlook 2040*; Organization of the Petroleum Exporting Countries: Vienna, Austria, 2019.
2. Zhao, F.; Liu, Y.; Lu, N.; Xu, T.; Zhu, G.; Wang, K. A review on upgrading and viscosity reduction of heavy oil and bitumen by underground catalytic cracking. *Energy Rep.* **2021**, *7*, 4249–4272. [[CrossRef](#)]
3. Zhang, X.; Liu, Q.; Fan, Z.; Liu, Y. Enhanced heavy oil recovery and performance by application of catalytic in-situ combustion. *Pet. Sci. Technol.* **2019**, *37*, 493–499. [[CrossRef](#)]
4. Rocha, J.W.S.; Vicente, M.A.; Melo, B.N.; de Lourdes, S.P.; Marques, M.; Guimarães, R.C.L.; Sad, C.M.S.; Castro, E.V.R.; Santos, M.F.P. Investigation of electrical properties with medium and heavy Brazilian crude oils by electrochemical impedance spectroscopy. *Fuel* **2019**, *241*, 42–52. [[CrossRef](#)]
5. Li, Y.; Wang, Z.; Hu, Z.; Xu, B.; Li, Y.; Pu, W.; Zhao, J. A review of in situ upgrading technology for heavy crude oil. *Petroleum* **2021**, *7*, 117–122. [[CrossRef](#)]
6. Batlle, E.A.O.; Julio, A.A.V.; Santiago, Y.C.; Palácio, J.C.E.; Bortoni, E.D.C.; Nogueira, L.A.H.; Dias, M.V.X.; González, A.M. Brazilian integrated oilpalm-sugarcane biorefinery: An energetic, exergetic, economic, and environmental (4E) assessment. *Energy Convers. Manag.* **2022**, *268*, 116066. [[CrossRef](#)]
7. Alexandre, V.M.F.; de Castro, T.M.S.; de Araújo, L.V.; Santiago, V.M.J.; Freire, D.M.G.; Cammarota, M.C. Minimizing solid wastes in an activated sludge system treating oil refinery wastewater. *Chem. Eng. Process.* **2016**, *103*, 53–62. [[CrossRef](#)]
8. Vendramel, S.; Bassin, J.P.; Dezotti, M.; Sant’Anna, G.L. Treatment of petroleum refinery wastewater containing heavily polluting substances in an aerobic submerged fixed-bed reactor. *Environ. Technol.* **2015**, *36*, 2052–2059. [[CrossRef](#)]
9. González-Arias, J.; Carnicero, A.; Sánchez, M.E.; Martínez, E.J.; López, R.; Cara-Jiménez, J. Management of off-specification compost by using co-hydrothermal carbonization with olive tree pruning. Assessing energy potential of hydrochar. *Waste Manag.* **2021**, *124*, 224–234. [[CrossRef](#)]
10. Suárez Useche, M.A.; Castillo Santiago, Y.; Restrepo, J.B.; Albis Arrieta, A.R.; Agámez Salgado, K.P. Evaluation of the Zinc Sulfate Catalytic Effect in Empty Fruit Bunches Pyrolysis. *Processes* **2022**, *10*, 1748. [[CrossRef](#)]
11. Kim, S.W. Pyrolysis conditions of biomass in fluidized beds for production of bio-oil compatible with petroleum refinery. *J. Anal. Appl. Pyrolysis* **2016**, *117*, 220–227. [[CrossRef](#)]
12. Zhang, L.; Hu, X.; Li, C.; Zhang, S.; Wang, Y.; Esmaeili, V.; Gholizadeh, M. Fates of heavy organics of bio-oil in hydrotreatment: The key challenge in the way from biomass to biofuel. *Sci. Total Environ.* **2021**, *778*, 146321. [[CrossRef](#)] [[PubMed](#)]
13. Castillo Santiago, Y.; Pérez, J.F.; Sphaier, L.A. Reaction-front and char characterization from a palm kernel shell—Oil sludge mixture under oxygen lean regimes in a fixed-bed gasifier. *Fuel* **2022**, *333*, 126402. [[CrossRef](#)]
14. Castillo Santiago, Y.; Martínez González, A.; Venturini, O.J.; Sphaier, L.A.; Ocampo Batlle, E.A. Energetic and environmental assessment of oil sludge use in a gasifier/gas microturbine system. *Energy* **2022**, *244*, 123103. [[CrossRef](#)]
15. Watson, J.; Zhang, Y.; Si, B.; Chen, W.-T.; de Souza, R. Gasification of biowaste: A critical review and outlooks. *Renew. Sustain. Energy Rev.* **2018**, *83*, 1–17. [[CrossRef](#)]
16. Ghassemi, H.; Beheshti, S.M.; Shahsavan-Markadeh, R. Mathematical modeling of extra-heavy oil gasification at different fuel water contents. *Fuel* **2015**, *162*, 258–263. [[CrossRef](#)]
17. Yang, X.; Hamidzadeh, A.; Ilkhani, M.; Foroughi, A.; Esfahani, M.J.; Motahari-Nezhad, M. Aspen plus simulation of heavy oil gasification in a fluidized bed gasifier. *Pet. Sci. Technol.* **2016**, *34*, 1530–1533. [[CrossRef](#)]
18. Bader, A.; Hartwich, M.; Richter, A.; Meyer, B. Numerical and experimental study of heavy oil gasification in an entrained-flow reactor and the impact of the burner concept. *Fuel Process. Technol.* **2018**, *169*, 58–70. [[CrossRef](#)]
19. Banisaeed, M.; Rezaee-Manesh, A. A parametric study for gasification of liquid fuels. *Pet. Sci. Technol.* **2016**, *34*, 976–979. [[CrossRef](#)]
20. Zhang, X.; Wu, L.; Wang, X.; Ju, G. Comparative study of waste heat steam SRC, ORC and S-ORC power generation systems in medium-low temperature. *Appl. Therm. Eng.* **2016**, *106*, 1427–1439. [[CrossRef](#)]
21. Oyedepo, S.O.; Fakeye, B.A.; Mabinuori, B.; Babalola, P.O.; Leramo, R.O.; Kilanko, O.; Dirisu, J.O.; Udo, M.; Efemwenkikie, U.K.; Oyebanji, J.A. Thermodynamics analysis and performance optimization of a reheat—Regenerative steam turbine power plant with feed water heaters. *Fuel* **2020**, *280*, 118577. [[CrossRef](#)]
22. Ahmadi, M.H.; Alhuyi Nazari, M.; Sadeghzadeh, M.; Pourfayaz, F.; Ghazvini, M.; Ming, T.; Meyer, J.P.; Sharifpur, M. Thermodynamic and economic analysis of performance evaluation of all the thermal power plants: A review. *Energy Sci. Eng.* **2019**, *7*, 30–65. [[CrossRef](#)]
23. Dovichi Filho, F.B.; Castillo Santiago, Y.; Silva Lora, E.E.; Escobar Palacio, J.C.; Almazan del Olmo, O.A. Evaluation of the maturity level of biomass electricity generation technologies using the technology readiness level criteria. *J. Clean. Prod.* **2021**, *295*, 126426. [[CrossRef](#)]
24. Vaezi, M.; Passandideh-Fard, M.; Moghiman, M.; Charmchi, M. Gasification of heavy fuel oils: A thermochemical equilibrium approach. *Fuel* **2011**, *90*, 878–885. [[CrossRef](#)]
25. Safarian, S.; Ebrahimi Saryazdi, S.M.; Unnthorsson, R.; Richter, C. Gasification of Woody Biomasses and Forestry Residues: Simulation, Performance Analysis, and Environmental Impact. *Fermentation* **2021**, *7*, 61. [[CrossRef](#)]
26. ANP. *Anuário Estatístico Brasileiro do Petróleo, Gás Natural e Biocombustíveis*; ANP: Rio de Janeiro, Brazil, 2018.



27. Khessa, N.; Mulopo, J. Performance evaluation, Optimization and exergy analysis of a high temperature co-electrolysis power to gas process using Aspen Plus®—A model based study. *Energy Sci. Eng.* **2021**, *9*, 1950–1960. [CrossRef]
28. Tungalag, A.; Lee, B.; Yadav, M.; Akande, O. Yield prediction of MSW gasification including minor species through ASPEN plus simulation. *Energy* **2020**, *198*, 117296. [CrossRef]
29. Allegue, L.B.; Hinge, J. *Biogas Upgrading Evaluation of Methods for H2S Removal*; Danish technological institute: Taastrup, Denmark, 2014.
30. Marques, T.E.; Castillo Santiago, Y.; Renó, M.L.; Yepes Maya, D.M.; Sphaier, L.A.; Shi, Y.; Ratner, A. Environmental and Energetic Evaluation of Refuse-Derived Fuel Gasification for Electricity Generation. *Processes* **2021**, *9*, 2255. [CrossRef]
31. Ashizawa, M.; Hara, S.; Kidoguchi, K.; Inumaru, J. Gasification characteristics of extra-heavy oil in a research-scale gasifier. *Energy* **2005**, *30*, 2194–2205. [CrossRef]
32. de Oliveira Vilela, A.; Lora, E.S.; Quintero, Q.R.; Vicintin, R.A.; Pacceli da Silva e Souza, T. A new technology for the combined production of charcoal and electricity through cogeneration. *Biomass Bioenergy* **2014**, *69*, 222–240. [CrossRef]
33. Leme, M.M.V.; Venturini, O.J.; Lora, E.E.S.; Rocha, M.H.; Luz, F.C.; de Almeida, W.; de Moura, D.C.; de Moura, L.F. Electricity generation from pyrolysis gas produced in charcoal manufacture: Technical and economic analysis. *J. Clean. Prod.* **2018**, *194*, 219–242. [CrossRef]
34. Teixeira, M.A.; Escobar Palacio, J.C.; Sotomonte, C.R.; Silva Lora, E.E.; Venturini, O.J.; Aßmann, D. Assái—An energy view on an Amazon residue. *Biomass Bioenergy* **2013**, *58*, 76–86. [CrossRef]
35. Castillo Santiago, Y.; Martínez González, A.; Venturini, O.J.; Yepes Maya, D.M. Assessment of the energy recovery potential of oil sludge through gasification aiming electricity generation. *Energy* **2021**, *215*, 119210. [CrossRef]
36. Turner, M.J.; Pinkerton, L.L. *Quality Guidelines for Energy System Studies: Capital Cost Scaling Methodology*; National Energy Technology Laboratory: Pittsburgh, PA, USA, 2013.
37. Food and Agriculture Organization (FAO). *Bioenergy and Food Security Rapid Appraisal: User Manual*; FAO: Roma, Italy, 2014.
38. Holmgren, K.M. *Investment Cost Estimates for Gasificationbased Biofuel Production Systems*; IVL Swedish Environmental Research Institute: Stockholm, Switzerland, 2015.
39. Davidson, K.; Hite, R.; Jones, D.; Howley, A. *A Comprehensive Assessment of Small Combined Heat and Power Technical and Market Potential in California*; California Energy Commission: Sacramento, CA, USA, 2019.
40. Reyhani, H.A.; Meratizaman, M.; Ebrahimi, A.; Pourali, O.; Amidpour, M. Thermodynamic and economic optimization of SOFC-GT and its cogeneration opportunities using generated syngas from heavy fuel oil gasification. *Energy* **2016**, *107*, 141–164. [CrossRef]
41. Sagani, A.; Hagidimitriou, M.; Dedoussis, V. Perennial tree pruning biomass waste exploitation for electricity generation: The perspective of Greece. *Sustain. Energy Technol. Assess.* **2019**, *31*, 77–85. [CrossRef]
42. Valor Consulting Índice de Preços ao Produtor (IPP). Available online: <https://www.valor.srv.br/indices/ipp.php?pagina=1> (accessed on 28 October 2022).
43. Banco Central do Brasil Cotações e Boletins. Available online: <https://www.bcb.gov.br/estabilidadefinanceira/historicocotacoes> (accessed on 1 March 2022).
44. ANEEL. *Nota Técnica no 37/2019-SRM/ANEEL*; ANEEL: Brasília, Brazil, 2019.
45. Receita Federal do Brasil Tabela de Depreciação. Available online: <http://www.fazenda.rj.gov.br/sefaz/content/conn/UCMServer/uuid/dDocName%3AWCC201632> (accessed on 2 March 2022).
46. Han, J.; Liang, Y.; Hu, J.; Qin, L.; Street, J.; Lu, Y.; Yu, F. Modeling downdraft biomass gasification process by restricting chemical reaction equilibrium with Aspen Plus. *Energy Convers. Manag.* **2017**, *153*, 641–648. [CrossRef]
47. Martínez González, A.; Silva Lora, E.E.; Escobar Palacio, J.C.; Almazán del Olmo, O.A. Hydrogen production from oil sludge gasification/biomass mixtures and potential use in hydrotreatment processes. *Int. J. Hydrogen Energy* **2018**, *43*, 7808–7822. [CrossRef]
48. Upadhyay, D.S.; Sakhiya, A.K.; Panchal, K.; Patel, A.H.; Patel, R.N. Effect of equivalence ratio on the performance of the downdraft gasifier—An experimental and modelling approach. *Energy* **2019**, *168*, 833–846. [CrossRef]
49. Richardson, Y.; Drobek, M.; Julbe, A.; Blin, J.; Pinta, F. Biomass Gasification to Produce Syngas. In *Recent Advances in Thermo-Chemical Conversion of Biomass*; Pandey, A., Bhaskar, T., Stöcker, M., Sukumaran, R., Eds.; Elsevier: Boston, MA, USA, 2015; pp. 213–250. ISBN 978-0-444-63289-0.
50. Mohd Salleh, M.A.; Nsamba, H.K.; Yusuf, H.M.; Idris, A.; Karim, W.A.W.A.; Salleh, M.A.M.; Nsamba, H.K.; Yusuf, H.M.; Idris, A.; Wan Ab, W.A. Effect of Equivalence Ratio and Particle Size on EFB Char Gasification. *Energy Sources Part A Recover. Util. Environ. Eff.* **2015**, *37*, 1647–1662. [CrossRef]
51. Henaio, N.C.; Lora, E.E.S.; Maya, D.M.Y.; Venturini, O.J.; Franco, E.H.M. Technical feasibility study of 200 kW gas microturbine coupled to a dual fluidized bed gasifier. *Biomass Bioenergy* **2019**, *130*, 105369. [CrossRef]
52. Wang, M.; Wan, Y.; Guo, Q.; Bai, Y.; Yu, G.; Liu, Y.; Zhang, H.; Zhang, S.; Wei, J. Brief review on petroleum coke and biomass/coal co-gasification: Syngas production, reactivity characteristics, and synergy behavior. *Fuel* **2021**, *304*, 121517. [CrossRef]
53. Zoungrana, L.; Sidibé, S.D.; Herman, B.; Coulibaly, Y.; Jeanmart, H. Design of a Gasification Reactor for Manufacturing and Operation in West Africa. *Designs* **2021**, *5*, 76. [CrossRef]
54. Peng, W.X.; Wang, L.S.; Mirzaee, M.; Ahmadi, H.; Esfahani, M.J.; Fremaux, S. Hydrogen and syngas production by catalytic biomass gasification. *Energy Convers. Manag.* **2017**, *135*, 270–273. [CrossRef]

55. Couto, N.; Rouboa, A.; Silva, V.; Monteiro, E.; Bouziane, K. Influence of the Biomass Gasification Processes on the Final Composition of Syngas. *Energy Procedia* **2013**, *36*, 596–606. [[CrossRef](#)]
56. Odeh, N.; Harmsen, R.; Minett, S.; Edwards, P.; Perez-Lopez, A.; Hu, J. *Review of the Reference Values for High-Efficiency Cogeneration*; European Commission: Didcot, UK, 2015.
57. Arslan, O. Performance analysis of a novel heat recovery system with hydrogen production designed for the improvement of boiler effectiveness. *Int. J. Hydrogen Energy* **2021**, *46*, 7558–7572. [[CrossRef](#)]
58. Kalisz, S.; Pronobis, M.; Baxter, D. Co-firing of biomass waste-derived syngas in coal power boiler. *Energy* **2008**, *33*, 1770–1778. [[CrossRef](#)]
59. Craig, K.R.; Mann, M.K. *Cost and Performance Analysis of Biomass-Based Integrated Gasification Combined-Cycle (BIGCC) Power Systems*; National Renewable Energy Laboratory: Golden, CO, USA, 1996.
60. Ministério da Economia. *Tarifa Externa Comum (TEC)*; Governo do Brasil: Brasília, Brazil, 2019.
61. Presidência da República do Brasil. *Decreto no 9514/2018*; Governo do Brasil: Brasília, Brazil, 2018.
62. Presidência da República do Brasil. *Lei no 13137/2015*; Governo do Brasil: Brasília, Brazil, 2015.
63. Governo do Estado de Minas Gerais. *Decreto no 43080/2002*; Governo de MG: Belo Horizonte, Brazil, 2002.